IEEE Access
Multidisciplinary | Rapid Review | Open Access Journal

Received August 24, 2021, accepted September 6, 2021, date of publication September 10, 2021,
date of current version September 17, 2021.

Digital Object Identifier 10.1109/ACCESS.2021.3111611

Shape Characteristic Analysis of Chaotic Attractors for Leakage Current Signal of Ice-Covered Insulator

ALI HUI AND WEIQIANG LU
School of Electrical and Control Engineering, Xi'an University of Science and Technology, Xi'an 710054, China
Corresponding author: Weiqiang Lu (luredeer@163.com)

ABSTRACT The change and development of leakage current (LC) during the flashover process of insulators are closely related to the discharge process. Characteristic quantities of LC play an important role in the identification and prediction of ice-covered flashover development stages. In this paper, the feature extraction method for LC of ice-covered insulator is discussed based on the shape characteristics of chaotic attractor. Firstly, the power spectrum and the largest Lyapunov exponent are used to analyze the LC of ice-covered insulator qualitatively and quantitatively, which confirmed positive chaotic features during the flashover process. On this basis, the LC is reconstructed in phase space. To solve the problem that the attractor in the high-dimensional space cannot be observed in the phase space reconstruction, the principal vector analysis method is used to project the high-dimensional reconstruction vector into the three-dimensional space to reduce the dimension. Finally, the evolution law of chaotic attractor in each stage of LC under different pollution degree is analyzed and discussed. The results show that the LC of ice-covered insulator has obvious characteristics of attractor shape at different stages of pollution, and is sensitive to the degree of pollution and each stage of development. So the shape of the attractor of LC has important application value for the identification of pollution flashover state and prediction of pollution flashover process of ice-covered insulators.

INDEX TERMS Ice-covered insulator, leakage current, phase space reconstruction, principal vector analysis, chaotic attractor.

I. INTRODUCTION

The ice flashover accident caused by the insulator icing is one of the main reasons for the insulator fault. The research on the icing characteristics and flashover characteristics of insulators have important theoretical significance and practical value [1]. At present, it is generally believed that icing is a special form of pollution. The flashover of ice-covered insulators is similar to pollution discharge, which is also caused by leakage current (LC). The change and development of LC is one of the main factors leading to whether the ice-covered insulators can develop into a complete flashover [2]. LC is the result of a combination of multiple factors, such as water mist, frost, voltage level and pollution degree [3]. Therefore, obtaining the characteristic values reflecting the operation state of insulators in the LC can accurately predict the pollution flashover level and pollution flashover state of insulators, and provide a reliable reference for on-line monitoring of ice flashover of insulators on transmission lines.

In order to extract features that can reflect the essence of ice flashover from complex LC signal, researchers have done a lot of work and proposed a variety of feature extraction methods, including empirical mode decomposition ((EMD)) [4]–[6], ensemble empirical mode decomposition (EEMD) [7], [8], wavelet transform (WT) [9], [10], and harmonic analysis (HA) [11]–[13]. These methods are all suitable for the analysis of LC non-stationary signals, but the EMD has the defect of mode aliasing. Although the improved EEMD can solve the modal aliasing phenomenon, the calculation time becomes longer and the reconstruction error becomes larger [14]. The WT method has the problem that the number

The associate editor coordinating the review of this manuscript and approving it for publication was Dazhong Ma.

of decomposition layers is uncertain. For different fault conditions, the optimal number of decomposition layers is difficult to directly obtain [15]. The HA method mainly uses fast fourier transform (FFT) to extract useful information about the pollution degree and flashover process of insulators. In [11], the ratio of the fifth harmonic to the third harmonic is extracted by FFT, so as to study the fault characteristics of insulator LC. On the basis of [12], it is proposed to use the ratio of fifth and seventh harmonics together to third harmonics for fault feature extraction, which improves the accuracy of fault feature extraction. Reference [13] proposes to use the ratio of the sum of the harmonics of the LC at the frequency of 0–100 Hz to the frequency of 150–500 Hz as feature extraction, where analyzes the relationship between the ratios under different voltage levels. Although the HA method is simple and fast in the feature extraction of LC and the accuracy of feature extraction is constantly improving, there is still no unified standard for harmonic selection, which cannot completely match the discharge activity on the surface of the insulator.

In fact, for this kind of nonlinear LC with complex influencing factors, nonlinear time series analysis (such as chaos, fractal theory.) is the research method that can better describe essential characteristics and inherent changes. The theory holds the one-dimensional time series contains a wealth of system information and contains traces of all other variables involved in the dynamic changes of system [16]. For example, the phase space reconstruction of the one-dimensional time series provides a simple and effective method to obtain dimension information from the univariate time series. At present, the researchers have paid more and more attention to the evaluation and analysis of time-varying nonlinear and non-stationary systems by using the characteristic parameters of chaotic systems, which have been applied in the fields such as machinery [17], electricity [18], electronic circuits [19] and image encryption [20]. Reference [17] proposed a research method for the mechanical fault diagnosis of high-voltage circuit breakers based on phase space reconstruction, which carried out feature identification of circuit breaker switch faults. Reference [18] proposed a method for analyzing LC of ice-covered insulators based on feature extraction of correlation dimensions. Reference [19] proposed an electronic circuit design method based on chaos theory, which verified preliminary application through actual wireless transmission robots. These methods have applied chaos theory to related research and achieved certain results. Compared with the traditional signal processing method, the main advantage lies in the more accurate discussion of the complexity and internal characteristics of the signal, but the problems that follow are the high complexity of the calculation, the long operation time and the practical application in the exploratory stage. Therefore, chaos theory should be further studied in the LC analysis of ice-covered insulators.

In this paper, firstly, it is verified that whether the nonlinear and non-stationary signals of LC of ice-covered insulator have chaotic characteristics. Secondly, the phase space reconstruction technology is used to reconstruct the one-dimensional time signal of the LC into a high-dimensional phase space to fully expand complex features. In order to solve the problem that the attractor in high dimensional space cannot be observed in phase space reconstruction, We propose to use the main feature analysis method to solve the problem. Finally, the relationships between the shape characteristics of the attractors and the stages of flashover in the three-dimensional phase space are analyzed in detail. It is expected to provide reference for the insulator's extraction of pollution flashover characteristics and the prediction of pollution flashover process.

TABLE 1. Insulator Test Parameters.

Insulator Type	Height	Climbing distance	Diameter
XWP2−160 double umbrella	155 mm	455 mm	300 mm

(a) (b)

FIGURE 1. Insulator monolithic sample and long string experiment diagram. (a) Single piece double umbrella sample insulator. (b) Long string insulator experiment diagram.

II. TEST EQUIPMENT AND TEST METHODS

A. TEST DEVICE

The test was carried out in the large-scale environmental climate laboratory of the ultra-high voltage (UHV) AC test base, where ice flash characteristics were mainly studied for the typical long string insulation of 500 kV transmission lines. The test uses 28 pieces of XWP2-160 double umbrella insulator string. Insulator parameters are shown in Table 1.

Insulator monolithic samples and long string experiments are shown in Fig. 1. Voltage regulation control is carried out through YDTCW-6000 kVA/3×500 kV test transformer and the detection signal is connected to the ground wire in series to measure the LC signal. After signal conditioning and A/D conversion, it is input to the industrial control computer for storage and analysis. The NI USB-9215A (4 channels

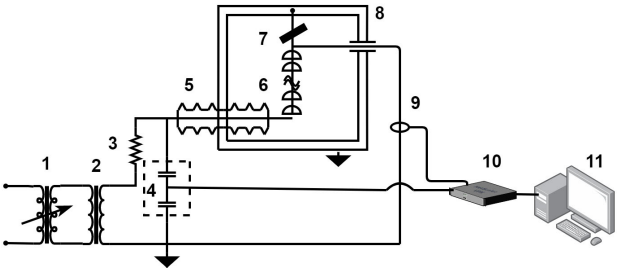

FIGURE 2. Wiring diagram of insulator AC icing flashover test.

16-bit simultaneous sampling input, the highest sampling rate is 100 kHz/s)data acquisition card simultaneously collects voltage and current signals. The LC sampling frequency is 10 kHz. The schematic diagram of the test wiring is shown in Fig. 2. Which includes 1. Column voltage regulator; 2. Test transformer; 3. Protection resistance; 4. Voltage divider; 5. Wall bushing; 6. Insulator string; 7. Analog transverse load; 8. Environmental Climate Laboratory; 9. LC sensor; 10. Data acquisition card; 11. Industrial computer.

B. TEST SAMPLE LAYOUT AND TEST METHOD

At present, there is no unified standard for the flashover test of insulator icing. Icing test method used in this paper draws on the existing icing methods, combined with the artificial pollution test method in IEC 60507:1991. The operations such as simulating real-type layout of insulators and applying ice on live are carried out [21]. During the test, the conductivity of the ice-covered water is 100 μS/cm at 20°C. In order to prevent the dirt on the insulator from being washed away when the water is first sprayed and iced, first use an artificial watering can to spray water mist on the upper and lower surfaces of the insulator to form a thin layer of ice protection. Then turn on the automatic water spray system to spray water and ice the insulator string. Finally, after the icing reaches a severe degree (the thickness of the bridging position of the icing is generally >20 mm), with the icing and the charging is stopped, the ice is frozen for more than 15 minutes to harden. After the icing is completed, the temperature inside the tank will rise rapidly to about −2°C, then the temperature rise rate will be controlled at 2 to 3°C/h. When there is a water film on the surface of the ice layer or there are water droplets falling on the ice edge, the test will be started at a rate of 8 kV/s. In the test, the lifting method is adopted to obtain the $U_{50\%}$ withstand voltage and the voltage level difference is selected about 5% according to the actual situation [1], [21].

The experiment simulates the samples with typical pollution degree respectively, and collects 10 sets of data for each group of samples. There are three groups of subjects in the experiment, which are taken according to the degree of pollution from heavy to light : ρ_{ESDD}/ρ_{NSDD} = 0.1/1.0 (mg/cm^2); ρ_{ESDD}/ρ_{NSDD} = 0.05/0.5 (mg/cm^2); ρ_{ESDD}/ρ_{NSDD} = 0.025/0.25 (mg/cm^2); Where ρ_{ESDD} means equivalent salt deposit density and ρ_{NSDD} means non-soluble deposit density. The collected LC waveforms under different pollution levels which are shown in Fig. 3 (a), (b), and (c).

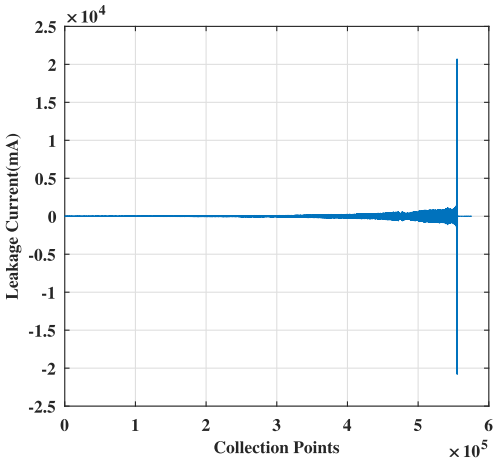

(a) LC waveform at ρ_{ESDD}/ρ_{NSDD} = 0.1/1.0 (mg/cm^2)

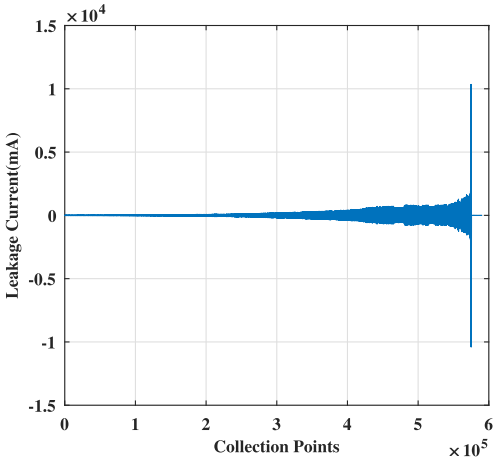

(b) LC waveform at ρ_{ESDD}/ρ_{NSDD} = 0.05/0.5 (mg/cm^2)

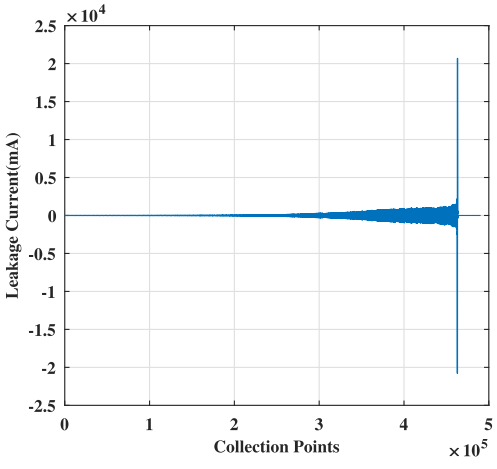

(c) LC waveform at ρ_{ESDD}/ρ_{NSDD} = 0.025/0.25 (mg/cm^2)

FIGURE 3. Leakage current waveform under different pollution levels.

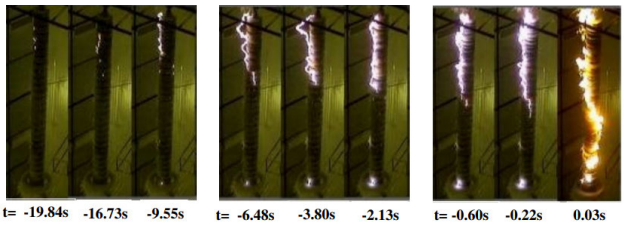

FIGURE 4. The whole process of 500kV insulator arc development.

C. ANALYSIS OF INSULATOR ICE FLASH PROCESS

The artificial ice coating experiment shows that after the ice-covered insulator applied the voltage, the LC will be generated. Take medium pollution degree $\rho_{ESDD}/\rho_{NSDD} = 0.05/0.5$ (mg/cm^2) as an example, Fig. 4 (a), (b), and (c) show the whole process of 500kV insulator from partial corona to flashover during ice melting.

1). 19.84s - 9.55s before flashover, a local arc will first be generated at the air gap of the insulator ice layer. There is a high-conductivity water film on the surface of the melted ice. The air gap bears most of the voltage, where the surrounding field strength is much higher than other parts. So the air gap is the starting point of insulator arc. Afterwards, the original local arc elongated and the number of local arc increased. (Fig. 4 (a)).

2). 6.48s-2.13s before flashover, the adjacent local arcs are gradually connected. After a period of time, the local arcs in the arc starting area are connected into a through white arc, which develops steadily along the surface of the remaining ice layer. During this stage, the LC increased significantly and the growth rate was significantly faster than the previous stage(Fig. 4 (b)).

3). 0.6s-0.22s before flashover, When the white arc reaches a certain length, the remaining ice layer cannot withstand the applied voltage and flashover occurs along the ice surface. The white arc becomes thicker and brighter, and the development length of the arc is greater than 2 / 3 of the string length, which may flashover at any time.(Fig. 4 (c)).

4). At the moment of flashover (0.03s), the LC increases instantly before the flashover. At this time, the arc quickly penetrates the entire insulator string and flashover occurs along the surface(Fig. 4 (c)).

Looking at the entire ice flash process of the pillar insulator this time, the LC varies from 20 to 1400 mA from the start of discharge to the instant of flashover. The entire ice melting flash process can be roughly divided into four stages: corona discharge, intermittent local arc, impending lightning arc, and flashover transient arc. Since the flashover moment is very short and the protection device will brake immediately at the flashover moment, the impending lightning arc and the flashover moment arc are treated in the same stage. According to the different development states of the above arc, the LC is finally divided into the initial stage, the development stage and the impending flash stage for analysis.

III. PHASE SPACE RECONSTRUCTION OF LC OF ICE-COVERED INSULATORS

In order to extract more useful information from time series, Packard *et al.* proposed the coordinate delayed reconstruction method for phase space reconstruction of time series [22]. The m-dimensional phase space vector is constructed by different delay time τ of one-dimensional time series $x(i)$. At the same time, according to the Takens embedding theorem, any D-dimensional hyperplane can be transformed into an equivalent Euclidean space with a corresponding dimension of m by being differentially embedded. Under the condition of $m \geq 2D + 1$, the reconstructed phase space maintains the topological characteristics and geometric invariance of the original attractor [23]. The specific principle is to assume that the time series of insulator LC as $x = \{x_{(i)}, i = 1, 2, \ldots, N\}$, where N is the length of time series. The m-dimensional phase space reconstructed from one-dimensional time series can be expressed as in (1):

$$\mathbf{x}_l = \begin{bmatrix} x_{(1)} & x_{(2)} & \cdots & x_{(l)} \\ x_{(1+\tau)} & x_{(2+\tau)} & \cdots & x_{(l+\tau)} \\ \vdots & \vdots & \vdots & \vdots \\ x_{(1+(m-1)\tau)} & x_{(2+(m-1)\tau)} & \cdots & x_{(l+(m-1)\tau)} \end{bmatrix} \tag{1}$$

where, $l = N-(m-1)\tau$, τ is the delay time(DT) and m is the embedding dimension(ED). Each column in (1) constitutes a phase point in the m-dimensional phase space, the connection between the l phase points describes the trajectory of the system in the m-dimensional phase space.

For an ideal infinite and noise-free one-dimensional time series, ED and DT can take multiple values. However, the actual LC has limited length and noise, it is necessary to calculate appropriate τ and m to realize the phase space reconstruction. According to the collected LC as the observation sequence of ice-covered insulators, the calculation methods of phase space DT and ED of the system are described respectively.

A. SELECTION OF DELAY TIME

The size of the DT determines the correlation between the various components of the LC. If τ is too small, the LC signal in the reconstructed phase space will be compressed, so that the dynamic characteristics of the system cannot be fully expanded; if τ is too large, the signal will be dispersed in the reconstructed phase space, and the LC signal will be seriously lost. At present, there are three main methods for determining the optimal delay time τ for reconstruction: autocorrelation function method(AFM) [24], average displacement method(ADM) [25] and mutual information method(MIM) [26]. Among them, the AFM is a description of the linear correlation of data, which is essentially not suitable for the analysis of nonlinear time series [27]. The ADM is a geometric method, in which the slope of the function drops to 40% of the initial value is taken as the best delay. This method has a certain degree of arbitrariness and its results are related to the selection of the m. The joint algorithm formed by it requires repeated experiments until the results are consistent, which is more cumbersome [27].

The first local minimum of the MIM function is used as the best delay method, and the theoretical foundation is perfect. It can be selected independently of the m, which is ideal. Therefore, this paper uses this method to calculate the DT.

Time series of LC of ice-covered insulator is $x = \{x_{(i)}, i = 1, 2, \ldots, N\}$. After the delay time τ, it is recorded as $x=\{x_{(i+\tau)}, i = 1, 2, \ldots, N\}$. Then the mutual information of x and x_τ can be defined by Shannon information entropy and probability distribution as in (2):

$$I_{(\tau)} = \sum_i P(x_{(i)}, x_{(i+\tau)}) \log_2 \frac{P(x_{(i)}, x_{(i+\tau)})}{P(x_{(i)}, P(x_{(i+\tau)})}. \quad (2)$$

where, $P(x_{(i)})$ is the probability of $x_{(i)}$ appearing in time series; $P(x_{(i+\tau)})$ is the probability of $x_{(i+\tau)}$ appearing in delayed time series; $P(x_{(i)}, x_{(i+\tau)})$ is the joint probability of appearing together in two series. The delay time and mutual information curve are calculated and drawn by (2). The DT of the first minimum of the curve is selected as the best for phase space reconstruction. As shown in Fig. 5, the delay time τ corresponding to the first local minimum of the mutual information function under different conditions is calculated as the DT in phase space reconstruction. The specific value of DT is shown in Table 2.

B. SELECTION OF EMBEDDED DIMENSION

When m is too small, the points that are originally far apart become very close in the reconstructed phase space, and the attractors are kinked and overlapped in the reconstructed phase space. When m is too large, since the dimensionality of noise is infinite, the error will occupy the entire reconstructed phase space. In this paper, the Cao method [28] is used to solve the ED, which is based on the idea of pseudo-neighbors. If d is the ED, then the two points in the d-dimensional space should also be included in the $d + 1$ dimensional space. Such points are called true neighboring points, otherwise they are pseudo neighboring points. The Cao method definition in (3), (4), and (5):

$$a(i, m) = \frac{\| y_i(m + 1) - y_{n(i,m)}(m + 1) \|}{\| y_i(m) - y_{n(i,m)}(m) \|}. \quad (3)$$

$$E(m) = \frac{1}{N - m\tau} \sum_{i=1}^{N-m\tau} a(i, m). \quad (4)$$

$$E_1(m) = \frac{E(m)}{E(m + 1)}. \quad (5)$$

where,$i = 1, 2, \ldots, N - m\tau$, $\| \blacksquare \|$ is Euclidean distance, $y_i(m+1)$ is the ith reconstructed space phasor, $y_{n(i,m)}(m+1)$ is the nearest point of $y_i(m + 1)$, $a(i, m)$ is relative increment of distance, $E(m)$ is the average distance between each point under the ED. Cao found that the $E_1(m)$ no longer changes (the threshold is 1% or 5%) when m is larger than a certain m_0. So $m_0 + 1$ is the minimum ED of the sequence. Still taking the data in Fig. 3, on the basis of determining the optimal DT, the pseudo-proximity method is used to calculate the ED respectively. Plot the relationship between the

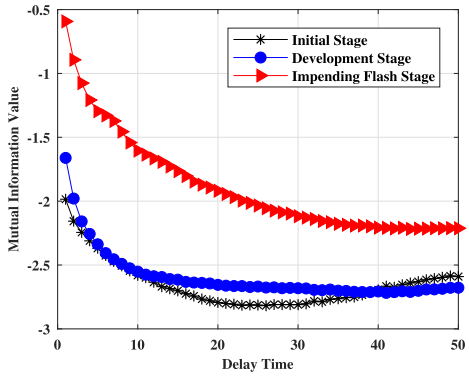

(a) DT curve at ρ_{ESDD}/ρ_{NSDD} = 0.1/1.0 (mg/cm^2)

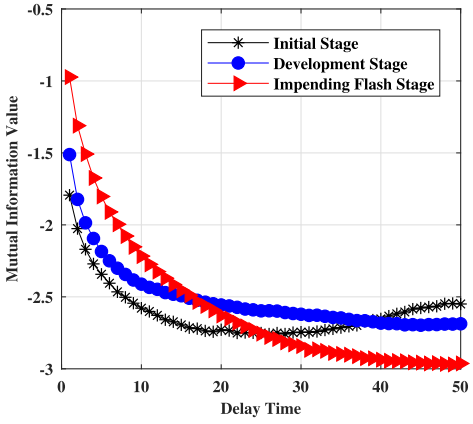

(b) DT curve at ρ_{ESDD}/ρ_{NSDD} = 0.05/0.5 (mg/cm^2)

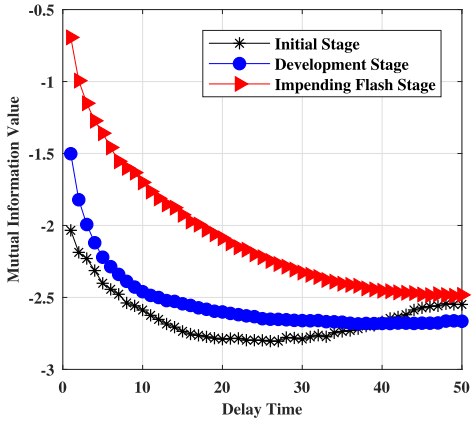

(c) DT curve at ρ_{ESDD}/ρ_{NSDD} = 0.025/0.25 (mg/cm^2)

FIGURE 5. Delay time curve of each stage under different pollution degree.

percentage of pseudo-nearest neighbors and the ED is shown in Fig. 6.

It is obvious in Fig. 6 that the percentage of pseudo-nearest neighbors tends to remain unchanged (the selection threshold in this paper is 5%), when the ED is greater than a certain value. Therefore, when the delay time τ is determined, the optimal ED of insulator LC at each stage can

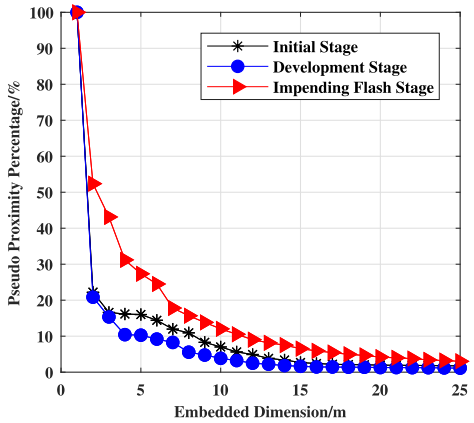

(a) ED curve at ρ_{ESDD}/ρ_{NSDD} = 0.1/1.0 (mg/cm^2)

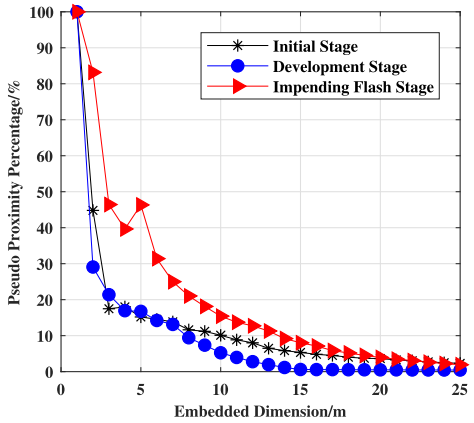

(b) ED curve at ρ_{ESDD}/ρ_{NSDD} = 0.05/0.5 (mg/cm^2)

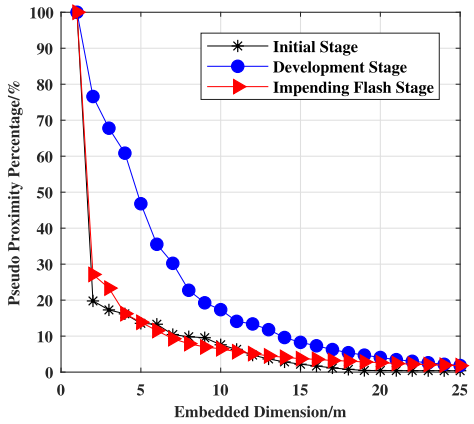

(c) ED curve at ρ_{ESDD}/ρ_{NSDD} = 0.025/0.25 (mg/cm^2)

FIGURE 6. ED curve of each stage under different pollution degree.

be determined. The specific values of the ED are shown in Table 2.

IV. ANALYSIS OF CHAOTIC CHARACTERISTICS OF LC

Phase space reconstruction is to reconstruct one-dimensional chaotic time series into high-dimensional phase space to extract and restore the original laws of the dynamic system. Therefore, it is necessary to judge whether the insulator breaking LC has chaotic characteristics first, then analyze it by phase space reconstruction technology. Commonly used methods to distinguish whether a system has chaotic characteristics mainly include qualitative methods (such as phase diagram method, power spectrum method) and quantitative methods (such as correlation dimension, Kolmogorov entropy and Lyapunov index). In this paper, the power spectrum method and largest Lyapunov exponent(L_{max}) are used to analyze the qualitative and quantitative chaotic characteristics of the ice-covered insulators.

TABLE 2. Table of values for each stage of DT and ED.

Stage		Initial		Development		Impending flash	
DT	ED	τ	m	τ	m	τ	m
0.1/1.0 (mg/cm^2)		23	18	24	17	37	20
0.05/0.5 (mg/cm^2)		19	19	25	16	31	24
0.025/0.25 (mg/cm^2)		20	20	31	24	46	15

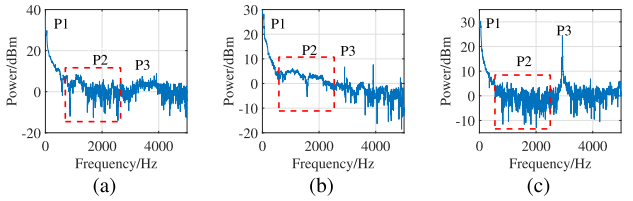

FIGURE 7. Power spectrum of LC.

A. POWER SPECTRUM ANALYSIS OF LC

It seems that the one-dimensional LC of ice-covered insulator is irregular, but its power spectrum can reflect a certain law. The power spectrum of time series with chaotic characteristics have the characteristics of continuity, wide peak and so on [29]. Taking the data in the Fig. 3, its power spectrum is shown in Fig. 7(a), (b), and (c).

It can be observed from the figure that the power spectrum of different LC has significant low (P1), medium (P2) and high (P3) frequency components. Their trends are broadly similar, especially in terms of low and high frequency components. The medium frequency components, as shown by the red dashed line, are quite different. All these indicate that: 1) The three main frequency components (P1, P2, and P3) are included for different levels of LC; 2) medium frequency components and high frequency components (P2 and P3) are more sensitive to changes in the state of ice-covered insulators than low frequency components (P1); 3) Leakage current signal contains quasi-periodic components; 4) Leakage current signal has chaotic characteristics.

TABLE 3. L_{max} in each stage of different pollution levels.

Stage	Initial	Development	Impending flash
$L_{max}(\times 10^{-3})$	$L1$	$L2$	$L3$
0.1/1.0 (mg/cm^2)	1.50	0.65	2.00
0.05/0.5 (mg/cm^2)	1.30	1.30	1.90
0.025/0.25 (mg/cm^2)	0.71	0.39	1.40

B. LARGEST LYAPUNOV EXPONENT OF LC SIGNAL

Being extremely sensitive to initial conditions is the basic feature of chaotic motion. The Lyapunov exponent is one of the important evaluations to quantitatively describe whether the nonlinear time series has chaotic characteristics. It is used to describe the exponential separation of two orbits with very close initial values over time. L_{max} determines the speed of the orbital divergence that covers the entire attractor. When L_{max} is positive, it indicates that the system has chaotic characteristics and the larger L_{max} indicates the faster the orbit divergence [30].

In this paper, the Wolf method [31] is used to calculate the L_{max}. Wolf method is characterized by no noise in time series and highly nonlinear evolution of small vectors in space. After calculation, the L_{max} of each stage of LC is greater than 0. The specific calculation results are shown in Table 3, which further proves that the LC of ice-covered insulator has chaotic characteristics.

V. SHAPE CHARACTERISTICS OF ATTRACTOR OF LC SIGNAL

In this section, the attractor shape characteristics of the LC are analyzed, including the shape characteristics of LC at the same pollution degree in different stages and the same stage. The analysis results are helpful to reveal the internal connection between insulator pollution flashover and chaotic attractor morphology, which provide a new idea to extract the characteristics of insulator flashover faults by using chaotic attractor signals.

A. PRINCIPAL VECTOR CHARACTERIZATION OF CHAOTIC ATTRACTOR

The one-dimensional time series is extended to the high-dimensional phase space by phase space reconstruction. Due to the limitation of cognition in high-dimensional space, attractors in high-dimensional space cannot be observed. Therefore, the principal vector analysis method [32] is used to project the high-dimensional reconstruction vector into the three-dimensional space. Three principal vectors are extracted from the reconstructed high-dimensional space and identified in three-dimensional space. The specific methods are as in (6) and (7). Find the inner product matrix Y of the reconstructed matrix X_l refering to (1):

$$Y = X_l^T X_l. \tag{6}$$

1) Calculate the eigenvalues of the inner product matrix Y select the three largest eigenvalues λ_1,λ_2,λ_3 as the three main eigenvalues.

2) Calculate the eigenvectors ξ_1,ξ_2,ξ_3, corresponding to the eigenvalues as the three main eigenvectors of the inner product matrix Y.

3) Project the reconstruction matrix X_l to the three principal vector directions to obtain an $N \times 3$ projection matrix Z:

$$\mathbf{Z} = X_l[\xi_1, \xi_2, \xi_3]. \tag{7}$$

Each row of the projection matrix Z represents the coordinate of a point. There are N such points in total. Connecting the coordinate points can get the shape of the attractor in the three-dimensional coordinate system. When the dimensionality reduction value is 3, the principal component variance contribution rate of each stage reaches more than 75%, and the average contribution rate under the same pollution degree is 88.54%, 90.71%, and 91.02%, which show that the method retains a large amount of original Information.

B. PHASE SPACE TRAJECTORY OF ATTRACTOR FOR LC SIGNAL OF ICE-COVERED INSULATOR

According to the above-mentioned principal vector analysis method, three groups of pollution degree initial stage, development stage, and impending flash stage are drawn separately in the three-dimensional coordinate system, as shown in Fig. 8. It is obvious in Fig. 8 that the LC of ice-covered insulators has plain differences in the shape characteristics of attractors at different stages under the same pollution degree, while the shape characteristics of attractors at different stages are very similar and have certain regularity under different pollution degrees. The specific rules are as follows.

Under the same pollution level, the attractor of LC shows a trend of development from small to large and the attractor has obvious shape characteristics in each stage. In the initial stage of icing flashover, the LC on the insulator string is very small and the waveform is relatively stable, which is generally a sine wave. As shown in Fig. 8 (a), (d),and (g), the attractor is wrapped around a central trajectory as a whole in the phase space reconstruction. With the increase of the voltage level, the LC at steel corner of high-voltage end insulator is sharp, which causes the LC waveform to change suddenly at certain points, but it drops quickly in a short time. Therefore, there are several outward discrete curves in the attractor trajectory((shown in the red box)). At this time, the projection of the attractor trajectory on the (x, y) plane is approximately a ring and the value range is 10-1000. In the development stage, the LC further increases, at this time the development trend of waveform becomes complicated. The stream jets in air gap at tip of the ice edge have intermittent arc discharge and the ice melting phenomenon increase. Part of the energy supplied by power supply is used to keep the arc burning, part is used to melt ice. When the two parts of energy reach equilibrium, the arc is extinguished.

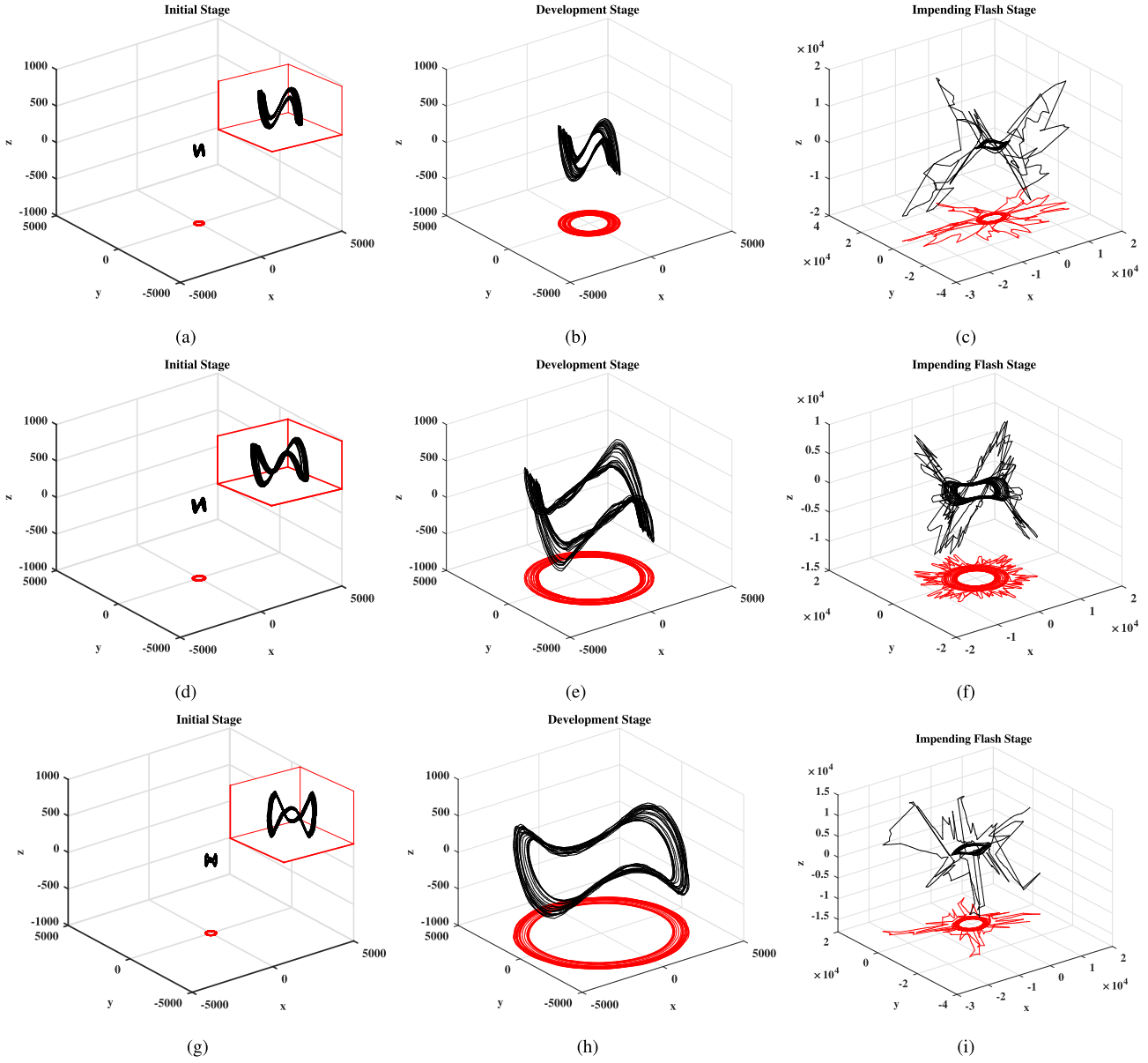

FIGURE 8. Shape characteristics of attractors at different stages of pollution. The red waveform is the projection of the attractor trajectory on the (x, y) plane. (a),(b),and(c) under ρ_E/ρ_N = 0.1/1.0 (mg/cm^2) condition. (d),(e),and(f) under ρ_E/ρ_N = 0.05/0.5 (mg/cm^2) condition. (g),(h),and(i) under ρ_E/ρ_N = 0.025/0.05 (mg/cm^2) condition.

The ice layer is further melted under the action of Joule heat of LC, the energy required for melting the ice is reduced. Then the conductive water film grows and the arc burns again. Fig. 8 (b), (e), and (h) are manifested that the discrete curves in the attractor trajectory further increase and the attractor trajectory overlaps or clusters in a certain track. The ring of the projection of the attractor trajectory on the (x, y) plane is further enlarged and the value range is between 1000-5000. In the impending flash phase, the Joule heat of the arc current can not only fully melt the ice layer, but also ensure that the intermittent arc burns stably and develops in air on the surface of the conductive water film. An arc appears between the insulator strings. As shown in Fig. 8 (c), (f), and (i), attractors will diverge outwards on the periphery of the central trajectory, constantly escaping from the central trajectory and then fall back into the trajectory. The complexity of the attractor track corresponds to the trend of arc development. The projection of the attractor trajectory on the (x, y) plane consists of two parts. The central part is a circular ring with a value range of 5000-8000; the edge part is a trajectory that escapes the central circular ring and its value is large and random.

Under different pollution levels, each stage has little effect on the position of the attractor's center trajectory. The attractors of the LC in the initial stage and the development stage have similar shapes and trajectories, while the impending

flash stage shows a certain degree of randomness. Because the arc characteristics in the initial stage and the development stage are not obvious. There is arc discharge, the ice melting absorbs a large amount of energy, but the arc discharge cannot continue to occur. In the impending flashover stage, the higher the pollution degree of the insulator(Fig. 8 (c)), the attractor trajectory mainly diverge in four directions. For insulators with low pollution(Fig. 8 (i)), the attractor trajectory shows divergence in all directions. This is the higher degree of pollution, the greater dominance of pollution in the whole ice-covered flashover process. The arc discharge generated by the air gap jet at the tip of the ice edge has relatively little effect. Therefore, the higher the pollution concentration, the more obvious divergence of the attractor trajectory in certain directions in the phase space.

Based on the above analysis, the chaotic analysis method for the LC of ice-covered insulators is closer to this complex system affected by multiple factors. Research shows that the trajectory of the chaotic attractor in each stage is obviously different and the trajectory of the attractor is more sensitive to the initial stage. Since the ice coating and melting process of insulators takes a long time, corresponding countermeasures can be taken in the initial stage of ice coating or melting according to the changing law of the attractor trajectory, which can prevent malfunctions such as short circuits and power outages caused by complete flashover. It can be applied to the fault prediction and processing of insulators in UHV transmission and transformation projects in high altitude areas. In the future, we will continue to analyze various types of insulators to enrich relevant research.

VI. CONCLUSION

Based on the ice accumulation and flashover test of the ceramic insulator string in cold climates under experimental conditions, the LC during the flashover process was measured. A method to identify the severity of flashover of ice-covered insulators is proposed based on the shape characteristics of chaotic attractors. It is proved that the LC has chaotic characteristics by analyzing thepower spectrum and the largest Lyapunov exponent. Phase space reconstruction and principal vector analysis are used to distinguish the shape characteristics of the chaotic attractor. The research results show that the chaotic attractor is highly sensitive to the severity of flashover of ice-covered insulators and the size of the attractor is highly correlated with the severity of flashover. The trajectory range of the attractor in the initial stage and the development stage is very small, while the range of the attractor in the impending flash stages is obviously larger, which is dozens of times as much as the initial stage and the development stage. The whole process presents a development trend from small to large, and there are intuitive and obvious differences in each stage. According to this phenomenon, the flashover threshold can be set as an early judgment for the insulator to enter the pollution flashover state.

REFERENCES

[1] X. Jiang, S. Wang, Z. Zhang, S. Xie, and Y. Wang, "Study on AC flashover performance and discharge process of polluted and iced IEC standard suspension insulator string," *IEEE Trans. Power Del.*, vol. 22, no. 1, pp. 472–480, Jan. 2007.

[2] M. Farzaneh, "Insulator flashover under icing conditions," *IEEE Trans. Dielectr. Electr. Insul.*, vol. 21, no. 5, pp. 1997–2011, Oct. 2014.

[3] Y. Hu, X. Jiang, Z. Yang, and X. Han, "Influence of crystallization effect during icing water phase transition on the flashover characteristics of ice-covered insulators," *IEEE Access*, vol. 8, pp. 176521–176529, 2020.

[4] S. Wang, "Fuzzy evaluation of insulator pollution flashover based on improved EMD de-noising and entropy weight method," *J. Inf. Comput. Sci.*, vol. 12, no. 15, pp. 5687–5696, Oct. 2015.

[5] Z. M. Shu and L. J. Zheng, "Insulator leakage current analysis based on time-frequency and HHT methods," in *Proc. 4th Int. Conf. Comput. Sci. Netw. Technol. (ICCSNT)*, Harbin, China, Dec. 2015, pp. 1365–1369.

[6] M. C. Yi, J. Fang, Y. Wang, Z. N. Li, C. H. Gu, N. Q. Shu, and Z. P. Li, "A method for extracting acoustic emission signal frequency characteristics of polluted-insulator discharge," *Appl. Mech. Mater.*, vols. 494–495, pp. 1513–1516, Feb. 2014.

[7] L.-M. Wei, J.-B. Sun, and Y.-L. Zhu, "A de-noising method based on EEMD for insulator leakage current," *J. North Chin. Electr. Power Univ.*, vol. 39, no. 2, pp. 17–22, Mar. 2012.

[8] M. Zhao, J. Liu, and Y. Wang, "Research on characteristics of leakage current based on improved HHT algorithm," in *Proc. CSEE*, Oct. 2016, vol. 36, no. 20, pp. 5657–5667.

[9] D. Maadjoudj, A. Mekhaldi, and M. Teguar, "Flashover process and leakage current characteristics of insulator model under desert pollution," *IEEE Trans. Dielectr. Electr. Insul.*, vol. 25, no. 6, pp. 2296–2304, Dec. 2018.

[10] X.-B. Huang, J.-Q. Li, Y. Zhang, and F. Zhang, "Recognition and detection technology of ice-covered insulators under complex environment," *High Voltage Eng.*, vol. 43, no. 3, pp. 891–899, Mar. 2017.

[11] M. F. Palangar and M. Mirzaie, "Detection of critical conditions in ceramic insulators based on harmonic analysis of leakage current," *Electr. Power Compon. Syst.*, vol. 44, no. 16, pp. 1854–1864, Oct. 2016.

[12] A. A. Salem, R. Abd-Rahman, H. Ahmad, M. S. Kamarudin, N. A. M. Jamal, N. A. Othman, and M. T. Ishak, "A new flashover prediction on outdoor polluted insulator using leakage current harmonic components," in *Proc. IEEE 7th Int. Conf. Power Energy (PECon)*, Kuala Lumpur, Malaysia, Dec. 2018, pp. 413–418.

[13] A. A. Salem, R. Abd-Rahman, S. A. Al-Gailani, M. S. Kamarudin, H. Ahmad, and Z. Salam, "The leakage current components as a diagnostic tool to estimate contamination level on high voltage insulators," *IEEE Access*, vol. 8, pp. 92514–92528, 2020.

[14] T. Dai, Y. Zhang, K. Zhang, B. He, H. Zhu, and J. Zhang, "The research progress of empirical mode decomposition and mode mixing elimination," *Appl. Electr. Tech.*, vol. 45, no. 3, pp. 7–12, 2019.

[15] M. A. Douar, A. Mekhaldi, and M. C. Bouzidi, "Flashover process and frequency analysis of the leakage current on insulator model under non-uniform pollution conditions," *IEEE Trans. Dielectr. Electr. Insul.*, vol. 17, no. 4, pp. 1284–1297, Aug. 2010.

[16] J. P. Eckmann and D. Ruelle, "Ergodic theory of chaos and strange attractors," *Rev. Mod. Phys.*, vol. 57, no. 3, pp. 273–312, 1985.

[17] Q.-Y. Yang, J.-J. Ruan, Z.-J. Zhuang, D.-H. Huang, and Z.-B. Qiu, "Vibration signature extraction of high-voltage circuit breaker by frequency and chaotic analysis," *IEEE Access*, vol. 7, pp. 80884–82892, 2019.

[18] Y. Liu, M. Farzaneh, and B. X. Du, "Using chaotic features of leakage current for monitoring dynamic behavior of surface discharges on an ice-covered insulator," *IEEE Trans. Dielectr. Electr. Insul.*, vol. 24, no. 4, pp. 2607–2615, Sep. 2017.

[19] S. Vaidyanathan, A. Sambas, M. Mamat, and W. M. Sanjaya, "A new three-dimensional chaotic system with a hidden attractor, circuit design and application in wireless mobile robot," *Arch. Control Sci.*, vol. 27, no. 4, pp. 541–554, Dec. 2017.

[20] A. Sambas, S. Vaidyanathan, E. Tlelo-Cuautle, B. Abd-El-Atty, A. A. A. El-Latif, O. Guille-Fernandez, Y. Hidayat, and G. Gundara, "A 3-D multi-stable system with a peanut-shaped equilibrium curve: Circuit design, FPGA realization, and an application to image encryption," *IEEE Access*, vol. 8, pp. 137116–137132, 2020.

[21] *Artificial Pollution Tests on High Voltage Insulators to be Used on A.C. Systems*, document IEC 60507, 1991.
[22] N. H. Packard, J. P. Crutchfield, J. D. Farmer, and R. S. Shaw, "Geometry from a time series," *Phys. Rev. Lett.*, vol. 45, no. 9, p. 712, Sep. 1980.
[23] Y. Zou, R. V. Donner, N. Marwan, J. F. Donges, and J. Kurths, "Complex network approaches to nonlinear time series analysis," *Phys. Rep.*, vol. 787, pp. 1–97, Jan. 2019.
[24] M. T. Rosenstein, J. J. Collins, and C. J. D. Luca, "Reconstruction expansion as a geometry-based framework for choosing proper delay times," *Physica D, Nonlinear Phenomena*, vol. 73, no. 1, pp. 82–89, May 1994.
[25] J. Zhang, Y.-Y. Fan, H. M. Li, H.-Y. Sun, and M. Jia, "An improved algorithm for choosing delay time in phase space reconstruction," *Chin. J. Comput. Phys.*, vol. 28, no. 3, pp. 469–474, May 2011.
[26] M. F. Andrew and L. S. Harry, "Independent coordinates for strange attractors from mutual information," *Phys. Rev. A, Gen. Phys.*, vol. 33, no. 2, pp. 1134–1154, Feb. 1986.
[27] S. Wallot and D. Mønster, "Calculation of average mutual information (AMI) and false-nearest neighbors (FNN) for the estimation of embedding parameters of multidimensional time series in MATLAB," *Frontiers Psychol.*, vol. 9, pp. 1134–1152, Sep. 2018.
[28] L. Cao, "Practical method for determining the minimum embedding dimension of a scalar time series," *Phys. D, Nonlinear Phenomena*, vol. 110, nos. 1–2, pp. 43–50, Dec. 1997.
[29] Q. Yang, J. Ruan, Z. Zhuang, and D. Huang, "Chaotic analysis and feature extraction of vibration signals from power circuit breakers," *IEEE Trans. Power Del.*, vol. 35, no. 3, pp. 1124–1135, Jun. 2020.
[30] W. Kinsner, "Characterizing chaos through Lyapunov metrics," *IEEE Trans. Syst., Man, C, Appl. Rev.*, vol. 36, no. 2, pp. 141–151, Mar. 2006.
[31] A. Wolf, J. B. Swift, H. L. Swinney, and J. A. Vastano, "Determining Lyapunov exponents from a time series," *Phys. D, Nonlinear Phenomena*, vol. 16, no. 3, pp. 285–317, 1985.
[32] H. Abdi and L. J. Williams, "Principal component analysis," *IEEE Trans. Power Del.*, vol. 2, no. 4, pp. 433–459, Jul. 2010.

ALI HUI was born in Pucheng County, Shaanxi, China, in 1975. She received the B.S. and M.S. degrees in control engineering from Xi'an University of Science and Technology, and the Ph.D. degree in control theory and engineering from Northwestern Polytechnical University, Xi'an, Shaanxi, in 2009.

From 2001 to 2003, she was a Research and Development Engineer with Great Wall Computer Company Ltd. Since 2009, she has been a Lecturer with the School of Electrical and Control Engineering, Xi'an University of Science and Technology. She is the author of more than 30 articles. Her research interests include signal proceeding, pattern recognizing, HV contaminated insulators flashover monitoring and risk prediction, and fault diagnosis of electrical equipment.

Dr. Hui was a recipient of the first prize of Coal Industry Association Award, in 2018.

WEIQIANG LU was born in Jiangsu, China, in 1994. He received the B.S. degree in electrical engineering and automation from Xi'an Jiaotong University City College, Xi'an, China, in 2018. He is currently pursuing the M.S. degree in electrical engineering with Xi'an University of Science and Technology. His current research interests include HV contaminated insulators flashover monitoring and fault diagnosis of motor.